Prospects for Measuring Rainfall Using Propagation Differential Phase in X- and K_a-Radar Bands

SERGEY Y. MATROSOV

Cooperative Institute for Research in Environmental Sciences, University of Colorado and NOAA/Environmental Technology Laboratory, Boulder, Colorado

ROBERT A. KROPFLI, ROGER F. REINKING, AND BROOKS E. MARTNER

NOAA/Environmental Technology Laboratory, Boulder, Colorado

(Manuscript received 9 February 1998, in final form 29 June 1998)

ABSTRACT

Model calculations and measurements of the specific propagation and backscatter differential phase shifts (K_{DP} and δ_o, respectively) in rain are discussed for X- ($\lambda \sim 3$ cm) and K_a-band ($\lambda \sim 0.8$ cm) radar wavelengths. The details of the drop size distribution have only a small effect on the relationships between K_{DP} and rainfall rate R. These relationships, however, are subject to significant variations due to the assumed model of the drop aspect ratio as a function of their size. The backscatter differential phase shift at X band for rain rates of less than about 15 mm h^{-1} is generally small and should not pose a serious problem when estimating K_{DP} from the total phase difference at range intervals of several kilometers. The main advantage of using X-band wavelengths compared to S-band ($\lambda \sim 10$–11 cm) wavelengths is an increase in K_{DP} by a factor of about 3 for the same rainfall rate. The relative contribution of the backscatter differential phase to the total phase difference at K_a band is significantly larger than at X band. This makes propagation and backscatter phase shift contributions comparable for most practical cases and poses difficulties in estimating rainfall rate from K_a-band measurements of the differential phase.

Experimental studies of rain using X-band differential phase measurements were conducted near Boulder, Colorado, in a stratiform, intermittent rain with a rate averaging about 4–5 mm h^{-1}. The differential phase shift approach proved to be effective for such modest rains, and finer spatial resolutions were possible in comparison to those achieved with similar measurements at longer wavelengths. A K_{DP}–R relation derived for the mean drop aspect ratio ($R = 20.5K_{DP}^{0.80}$) provided a satisfactory agreement between rain accumulations derived from radar measurements of the differential phase and data from several nearby high-resolution surface rain gauges. For two rainfall events, radar estimates based on the assumed mean drop aspect ratio were, on average, quite close to the gauge measurements with about 38% relative standard deviation of radar data from the gauge data.

1. Introduction

Attempting to improve radar estimates of rainfall through the use of multiparameter radar measurements has a long history (Atlas et al. 1984). Recently, however, there have been a number of experimental studies (e.g., Zrnic and Ryzhkov 1996; Ryzhkov and Zrnic 1996) indicating that radar rainfall rate estimators based on the specific differential propagation phase shift (K_{DP}) between horizontally and vertically polarized signals outperform widely used empirical relations between rainfall rate R and equivalent radar reflectivity Z_e (Z_e–R relations). Advantages of the differential phase approach are their independence of 1) the radar receiver and transmitter calibration, 2) the attenuation of radar signals in rain, and 3) a partial radar beam blockage. Most importantly, differential phase as a function of rain rate is less sensitive than reflectivity to the variations of the drop size distribution. Also, phase measurements are not biased by ground clutter cancelers.

Theoretical considerations of the differential phase approach to rainfall measurements can be traced back to the work of Seliga and Bringi (1978); however, extensive experimental studies have a more recent history. These studies were limited mostly to the S-band radar wavelengths, with some recent exceptions including C-band wavelengths (e.g., May et al. 1997). At long wavelengths such as S band (10–11 cm), the propagation differential phase shift is relatively small and estimations of rainfall rate require significant spatial and temporal averaging. This makes radar measurements of light to moderate rain difficult if possible at all. A recent

Corresponding author address: Dr. Sergey Y. Matrosov, CIRES, University of Colorado and NOAA/Environmental Technology Laboratory, 325 Broadway, R/E/ET6, Boulder, CO 80303.
E-mail: smatrosov@etl.noaa.gov

study by Blackman and Illingworth (1997) puts a minimal rain rate practically retrievable from S-band K_{DP} data at 7.5 mm h^{-1} for 5 km averaging at 25-km range. Measurements of K_{DP} at X band could lower limiting values by a factor of about 3.

In the Rayleigh scattering regime, the magnitude of K_{DP} is proportional to the reciprocal of the radar wavelength. Consequently, the use of shorter wavelengths will allow more accurate estimations of light to moderate rain and improve temporal and spatial resolution because of the greater phase change per unit rainfall rate.

Partial signal attenuation in rain, which is one of the major difficulties in applying traditional Z_e–R relations at short radar wavelengths, is not a problem for the differential phase approach unless radar signals suffer complete attenuation. Preliminary calculations show that deviations from the Rayleigh scattering for X-band wavelengths are expected to be small for light and moderate rain rates. These deviations, however, are more profound at K_u- and, especially, at K_a-band wavelengths.

One important complication that needs to be more carefully evaluated at shorter wavelengths is the differential phase shift on backscatter, a non-Rayleigh effect, that is a part of the total differential phase shift measured by polarization diversity radar. The backscatter phase shift cannot be readily separated from propagation phase shift and it increases with an increase in raindrop sizes. At S-band wavelengths, backscatter differential phase shift is usually very small compared to the propagation phase shift if estimates are done over the range of a few kilometers.

The Radar Meteorology and Oceanography Division of the NOAA/Environmental Technology Laboratory (ETL) has developed two polarization radars operating at X band ($\lambda = 3.2$ cm) and one at K_a band ($\lambda = 0.86$ cm). One of the two X-band radars was recently upgraded with a new data acquisition system (Campbell and Gibson 1997) and pulse-to-pulse transmitter polarization switching. It is now capable of K_{DP} as well as other linear polarization parameter measurements.

Published work, either theoretical or observational, on the use of differential phase measurements at wavelengths shorter than C-band wavelengths is limited, with a few exceptions (Jameson 1994a, 1991; Kezys et al. 1993; Tan et al. 1991). In this paper, we present the results of modeling propagation and backscatter differential phase shifts at X and K_a band in rain, estimate the variability of K_{DP}–R relations due to natural changes in drop shape and drop size distributions, and assess potentials for estimating light to moderate rainfall rates from K_{DP} measurements with X-band radars. Some initial data obtained with the ETL X-band radar in light rain are given to illustrate these potentials.

2. Propagation differential phase shift at X and K_a bands

The equation for the specific one-way differential phase shift due to propagation of radar signals at a wavelength λ through rain can be written as (Matrosov 1991)

$$K_{DP} = \frac{-\lambda^2}{2\pi} \int_0^{D_{max}} \mathrm{Im}[S_h(D_e) - S_v(D_e)] N(D_e)\, dD_e, \quad (1)$$

where S_h and S_v are forward-scattering amplitudes at horizontal (h) and vertical (v) polarizations, respectively, for a drop with the equal-volume diameter D_e, and $N(D_e)$ is the drop size distribution (DSD). The K_{DP} measure in (1) is radian per unit length. The amplitudes S_h and S_v are dimensionless and defined as in Bohren and Huffman (1983). They relate to the forward-scattering amplitudes f often used in the radar meteorology literature as $S_p = -2\pi i f_p/\lambda$, where p is the polarization subscript. In (1), we do not perform integration with respect to the particle canting angles because canting angle effects are very small compared to the variations in differential phase due to different models of drop shapes (i.e., drop aspect ratios). It was assumed in model calculations that $D_{max} = 7$ mm.

a. Models of raindrop shapes

The shape of falling raindrops is close to that of oblate spheroids, and their aspect ratio r decreases as D_e increases. The equilibrium shapes can be approximated by the empirical formula

$$a/b = 1.03 - 0.62 D_e \qquad (D_e > 0.05 \text{ cm}), \quad (2)$$

which provides aspect ratios close to the ones presented by Pruppacher and Pitter (1971). There are indications (e.g., Kubesh and Beard 1993), however, that oscillations of raindrops cause their mean shape to be less oblate than the equilibrium shape. Mean aspect ratios of oscillating raindrops given by Kubesh and Beard (1993) can be approximated by the formula in the form of (2) but with the coefficient 0.44 instead of 0.62. Note that the drop aspect ratio suggested by Morrison and Cross (1974),

$$a/b = (1 - \upsilon/3)/(1 + \upsilon/6)$$
$$(\upsilon = D_e - D_e^2/4, \text{ where } D_e \text{ is in cm}), \quad (3)$$

is between the mean and equilibrium shapes for $D_e > 2$ mm. The recent work of Bringi et al. (1998) also shows examples of droplets (2 mm $< D_e <$ 4 mm) being more spherical than the equilibrium shape suggests.

To assess the variability in differential phase due to drop shapes, we performed calculations with both equilibrium and mean aspect ratios. Figure 1 shows the product $(f_h - f_v)\lambda^2$ for individual drops as a function of their equal-volume diameter. The scaling factor λ^2 was included because the amplitudes f_h and f_v are proportional to λ^{-2} in the Rayleigh scattering regime. For comparisons, S-band data are also shown in this figure. Calculations of scattering amplitudes were performed using the T-matrix approach (Barber and Yeh 1975) for the horizontal incidence and the vertical orientation of drop axes. The complex refractive indices of water were calculated assuming a temperature of 10°C.

As seen in Fig. 1 the scattering amplitude behavior

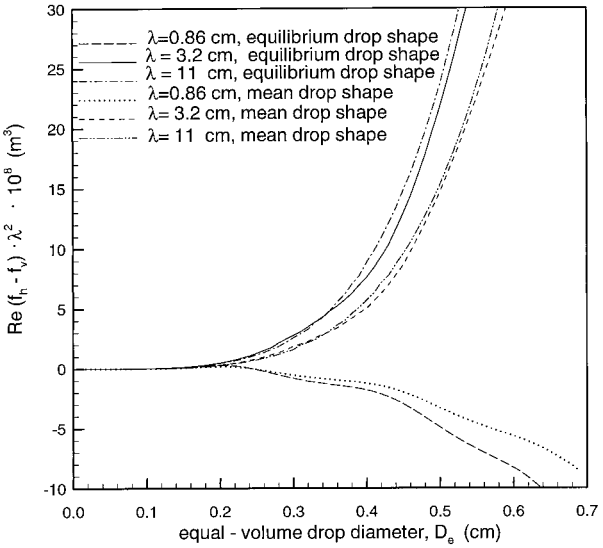

FIG. 1. Forward-scattering amplitude difference as a function of drop size for different radar wavelengths and drop shape models.

at S band is similar to that at X band, which means that K_{DP}–R relations would differ at those bands by, approximately, only a scaling factor of about 3 (i.e., the ratio of the wavelengths at those bands). On the other hand, scattering amplitudes at K_a-band exhibit a strongly non-Rayleigh behavior. First, the difference $f_h - f_v$ is positive, but then f_h becomes smaller than f_v for drop sizes greater than about 2.5 mm for both models of particle shapes. This means that potentially useful differential phase measurements at K_a band could be limited to very light rainfall rates.

b. Models of drop size distributions

Variability in K_{DP}–R relations due to DSD variations can be estimated in two ways: 1) calculating differential phase shift and rain rate for a model distribution when parameters of this distribution are allowed to vary in a priori-specified intervals and 2) calculating these parameters for experimental DSD. Following Chandrasekar et al. (1990), we assumed a gamma-function drop size distribution in the form of

$$N(D) = N_o D_e^n \exp[-(3.67 + n)D_e/D_m] \quad [\mathrm{L}]^{-4}. \quad (4)$$

The DSD simulations were performed for the order of the gamma-function n changing from -1 to 4 with the increment of 1, and the median volume diameter of drops D_m changing from 0.8 mm to 2 mm with the increment of 0.3 mm. As in Ryzhkov and Zrnic (1995), the parameter N_o (m^{-3} mm^{-1-n}), according to Ulbrich (1983), was allowed to vary in the interval specified by the choice of n: $10^{3.2-n} \exp(2.8n) < N_o < 10^{4.5-n} \exp(3.57n)$. Six equally spaced values of N_o were used in calculations for each D_m and n.

We also estimated the variability of K_{DP}–R relations using experimental data given by Sauvageot and Lacaux (1995). These authors published results of disdrometer measurements from several locations fitted by parameters σ, D_g, and N_T of the lognormal distribution

$$N(D) = N_T/[(2\pi)^{0.5} D_e \ln\sigma] \exp[-\ln^2(D_e/D_g)/(2\ln^2\sigma)] \quad [\mathrm{L}]^{-4}. \quad (5)$$

Although the use of these distributions for estimating the variability of K_{DP}–R relations does not substitute for the use of original disdrometer data, we performed calculations for the published distributions (5) in a manner similar to that of Ryzhkov and Zrnic (1996) in order to estimate sensitivity of these relations to the DSD type.

c. Sensitivity of K_{DP}–R relations to DSD and drop shape models

Calculations of the rainfall rate R for the DSD discussed above were made using the integral

$$R = \frac{\pi}{6} \int_0^{D_{\max}} D_e^3 v(D_e) N(D_e)\, dD, \quad (6)$$

where the drop terminal fall velocities (in m s^{-1}) were approximated by the polynomial fit suggested by Wobus et al. (1971):

$$\begin{aligned} v(r_e) &= 3.67 \times 10^{-10} r_e^3 - 3.27 \times 10^{-6} r_e^2 \\ &\quad + 9.57 \times 10^{-3} r_e + 0.121 \\ &\quad (r_e = D_e/2 > 500\ \mu\mathrm{m}), \\ v(r_e) &= 8.03 \times 10^{-3} r_e + 0.0135 \\ &\quad (200\ \mu\mathrm{m} \le r_e \le 500\ \mu\mathrm{m}), \quad \text{and} \\ v(r_e) &= 1.2 \times 10^{-4} r_e - 0.1645 \qquad (r_e < 40\ \mathrm{nm}). \end{aligned} \quad (7)$$

As mentioned earlier, the main advantage of measuring K_{DP} at shorter radar wavelengths is the possibility of getting a phase signal from light and moderate rainfalls that is large enough to measure compared to measurements at longer wavelengths where the signal could be too small for reliable estimates. Light to moderate rainfalls, however, are of great climatological importance because a significant fraction of total rain accumulation generally comes from rainfalls with $R < 15$ mm h^{-1}. Mazin (1989), for example, mentions that for the European part of Russia, with a probability of more than 90%, the mean rainfall rate R is less than 11 mm h^{-1} for short rains with duration of less than 1 h. For the longer duration rains this probability increases, reaching more than 99% for rains with duration of more than 3 h. For rains with duration of less than 1 h and more than 3 h, the mean rainfall rate is less than 5 mm h^{-1} with probabilities of about 30% and 90%, respectively. Even in the Tropics stratiform rain could account for 40% of total accumulation (Houze and Hobbs 1982).

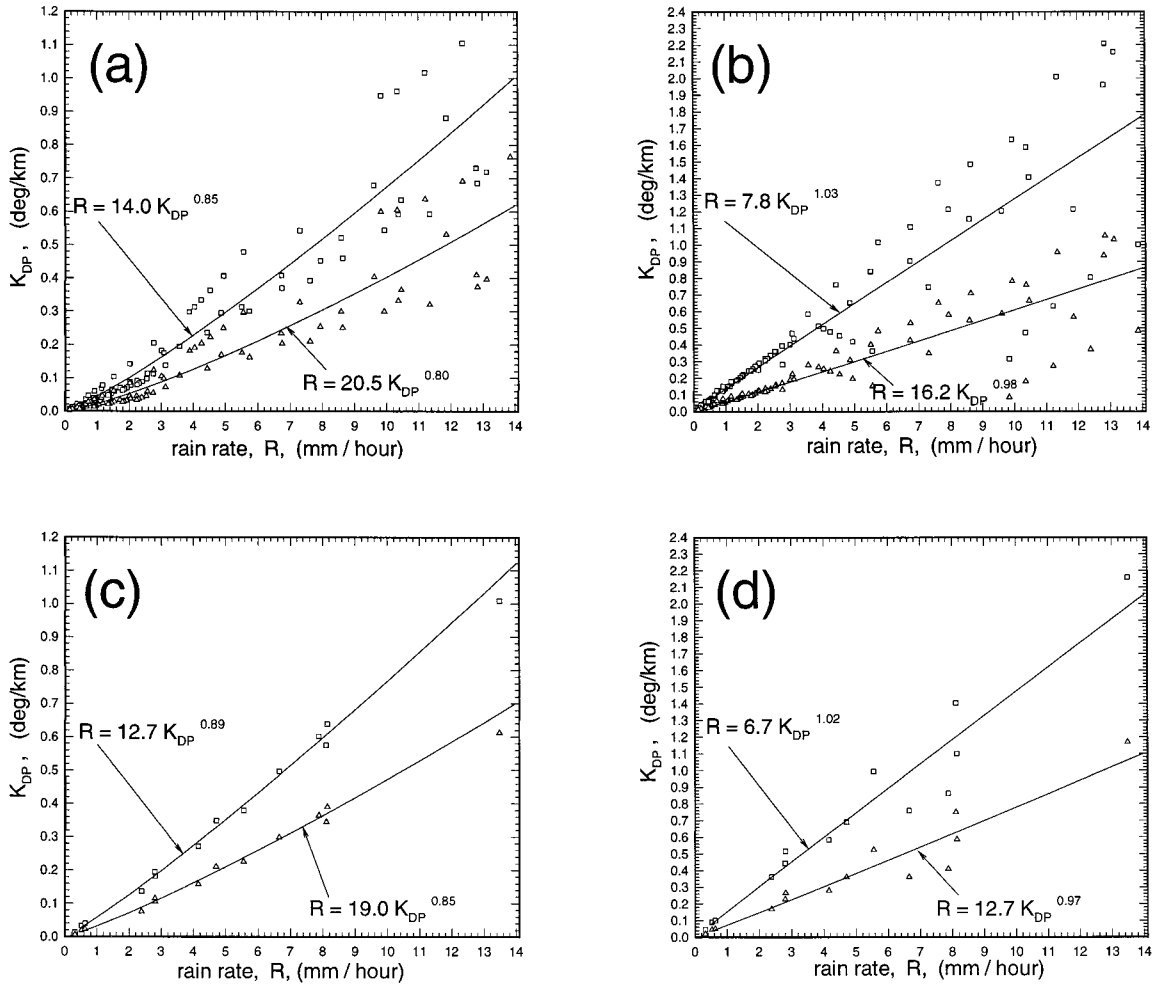

FIG. 2. Scatterplots of calculated K_{DP} vs rainfall rate: (a) and (c) $\lambda = 3.2$ cm; (b) and (d) $\lambda = 0.86$ cm; gamma DSD, (a) and (b); lognormal DSD, (c) and (d); squares, equilibrium drop shape; and triangles, mean drop shape.

Taking into account these considerations and the signal-to-noise advantages of shorter radar wavelengths over longer wavelengths for measuring light and moderate rains, we performed our calculations for rain rates $R <$ 15 mm h^{-1}.

Figure 2 shows the results of simulating K_{DP}–R relations for the gamma (Figs. 2a and 2b) and lognormal (Figs. 2c and 2d) distributions for the ETL radar wavelengths: $\lambda = 3.2$ cm and $\lambda = 0.86$ cm. Only DSD for which $R < 15$ mm h^{-1} were included. The coefficient a and the exponent b of the power-law regression fit,

$$R = aK_{DP}^{b}, \tag{8}$$

and the relative standard deviations of data from the best-fit curve are given in Table 1. This table also shows a and b values for $\lambda = 11$ cm (S band) and $\lambda = 5.3$ cm (C band) to allow comparison with published relations in these bands.

TABLE 1. Parameters and relative standard deviations of K_{DP}–R relations for $R < 15$ mm h^{-1}.

	Gamma distributions						Lognormal distributions					
	Equilibrium drop shape			Mean drop shape			Equilibrium drop shape			Mean drop shape		
	a	b	sd	a	b	sd	a	b	sd	a	b	sd
$\lambda = 0.86$ cm	7.8	1.03	23%	16.2	0.98	26%	6.7	1.02	14%	12.7	0.97	18%
$\lambda = 3.2$ cm	14.0	0.85	22%	20.5	0.80	30%	12.7	0.89	9%	19.0	0.85	12%
$\lambda = 5.3$ cm	21.6	0.84	23%	30.9	0.80	31%	20.2	0.89	9%	30.0	0.85	12%
$\lambda = 11$ cm	41.5	0.85	22%	58.1	0.80	30%	40.0	0.89	11%	59.1	0.86	12%

The best-fit power-law regressions for gamma and lognormal distributions are quite close, indicating a low sensitivity of K_{DP}–R relations to the type of DSD. The relative standard deviations of points about the best-fit curve, however, are significantly larger for model gamma distributions than for experimental distributions fitted by lognormal functions. This is probably because some combinations of the gamma-function parameters N_o, D_m, and n used in model calculations could be unrealistic. The relative standard deviations for both DSD types are significantly less (by a factor of 2 on average) than similar deviations for traditional Z_e–R relations that were also computed for the same drop size distributions (results are not shown). The Z_e–R relations were also quite sensitive to the type of DSD (gamma versus lognormal). Only 14 DSDs from Sauvageot and Lacaux (1995) data produced $R < 15$ mm h^{-1}. There is a need for more model DSD fits of disdrometer measurements to augment these data.

As seen in Fig. 2 and Table 1, K_{DP}–R relations are significantly more sensitive to the assumed drop aspect ratio (shape) model than to the details of DSD. Note that the exponent b does not change significantly, being around 1 for $\lambda = 0.86$ cm and around 0.85 for $\lambda = 3.2$ cm. The coefficient a, however, changes significantly, increasing by about 50% for $\lambda = 3.2$ cm and almost by a factor of 2 for $\lambda = 0.86$ cm when going from the equilibrium to the mean drop shape. This suggests that K_{DP}–R relations need tuning to select a proper value for a. Such tuning can be done by comparing gauge measurements of rainfall with estimates from radar differential phase measurements.

Values of the coefficient a and the exponent b for $\lambda = 11$ cm and equilibrium drop shape from Table 1 (corresponding figures are not shown) are very close to those used for the interpretation of National Severe Storm Laboratory's Cimarron radar ($\lambda = 10.97$ cm) K_{DP} measurements: $R = 40.6K_{DP}^{0.866}$ (Sachidananda and Zrnic 1987). Note that this relation was also derived for the equilibrium drop shape with the use of (2), and it was shown to provide results in a relatively good agreement with the surface rain gauge data especially for higher rain rates (Ryzhkov and Zrnic 1995). Note, however, that the C-band relation suggested by May et al. (1997), $R = 34.6K_{DP}^{0.83}$, is close to that obtained in this study for the mean drop aspect ratios and the corresponding radar wavelength ($\lambda = 5.3$ cm).

The results summarized in Table 1 for $\lambda = 3.2$ cm would not change significantly if a broader rain-rate interval were considered. Increasing this interval to 0–30 mm h^{-1} would decrease a only slightly to 12.1 and 18.2 for the equilibrium and mean drop shapes, respectively. The exponent b would not change effectively. This relative insensitivity of K_{DP}–R relations for $\lambda = 3.2$ cm to rain-rate interval is due to quasi-Rayleigh behavior of the forward-scattering amplitudes as a function of drop size at X band for the considered rain rates.

Calculations also indicated (results are not shown here) that the effects of incorporating the integration in (1) with respect to typical changes (a few degrees from the vertical) in the canting angle are significantly smaller than the ones caused by the uncertainties in drop aspect ratios as a function of size (i.e., equilibrium versus mean drop shapes). So these effects are neglected in subsequent considerations.

Rains with rates greater than 15 mm h^{-1} would likely contain larger drops. This could cause negative values of K_{DP} for $\lambda = 0.86$ cm because of the sign reversal of the scattering amplitude difference ($f_h - f_v$) as the characteristic size of raindrops increases (see Fig. 1). In Figs. 2a and 2c the data scatter around the best-fit regression becomes greater as rainfall rate increases. This scatter is low for $R < 3$ mm h^{-1}, while non-Rayleigh effects are relatively weak. The corresponding relative standard deviation for the K_a-band data diminishes by a factor of about 2 compared to values given in Table 1 if the rain-rate interval 0–3 mm h^{-1} is considered instead of the interval 0–15 mm h^{-1}.

3. Backscatter differential phase shift at X and K_a bands

The specific differential phase shift K_{DP} is estimated as a range derivative of the total differential phase shift φ_{DP} measured by radar. For non-Rayleigh scattering, there is also a contribution to φ_{DP} by the integrated differential phase shift on backscatter δ_o: $\varphi_{DP} = \varphi_{DP}^{(P)} + \delta_o$, where $\varphi_{DP}^{(P)}$ is the propagation phase shift. A simple estimation of K_{DP} is the slope of the total phase accumulation as a function of range between ranges r_1 and r_2:

$$K_{DP} = \frac{[\varphi_{DP}^{(P)}(r_2) - \varphi_{DP}^{(P)}(r_1)] + [\delta_o(r_2) - \delta_o(r_1)]}{2(r_2 - r_1)}. \quad (9)$$

In (9), the factor 2 in the denominator accounts for the fact that radar measures the two-way differential phase shift. The backscatter phase shift contaminates estimations of K_{DP} through the second term in the numerator. Values of δ_o are small for S-band wavelengths even for intense rainfall rates; however, the backscatter differential phase shift can cause some problems at X band. At K_a band, values of δ_o can be very significant even for modest rainfall rates.

Figure 3 shows the backscatter differential phase δ for individual drops as a function of drop size. As in the case of the propagation differential phase, calculations were performed for equilibrium and mean drop aspect ratios using the T-matrix algorithm. Here δ is defined as the difference between arguments of the complex backscatter amplitudes for horizontal (S_h^b) and vertical polarizations (S_v^b)

$$\delta = \arg(S_h^b) - \arg(S_v^b) = \arg[S_h^b(S_v^b)^*], \quad (10)$$

where (*) means complex conjugation.

As seen in Fig. 3 δ for $\lambda = 3.2$ cm remains very small for drops whose sizes do not exceed about 2–2.5

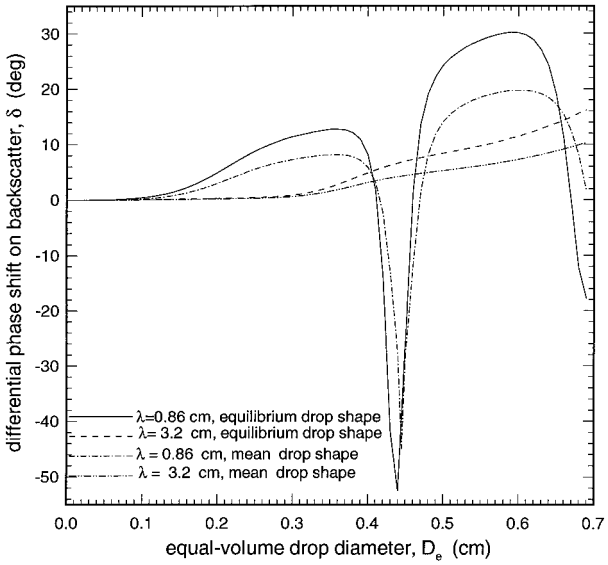

FIG. 3. Backscatter differential phase shift as a function of drop size for different radar wavelengths and drop shape models.

mm. For $D_e > 3$ mm, the rate of the δ increase with the drop size becomes more significant. This rate is greatest between $D_e = 3$ mm and $D_e = 4$ mm. The differential phase shift on backscatter at $\lambda = 0.86$ cm is very pronounced for drops with D_e larger than about 1 mm. It generally increases with the drop size increase for $D_e < 6$ mm except for the negative spike at about $D_e = 4.5$ mm.

The integrated backscatter phase shift for an ensemble of raindrops can be calculated by using the equation (Tan et al. 1991)

$$\delta_o = \arg\left[\int_0^{D_{\max}} S_{\mathrm{h}}^b(D_e)[S_{\mathrm{v}}^b(D_e)]^* N(D_e)\, dD_e\right]. \quad (11)$$

To estimate the variability of δ_o as a function of rain rate, calculations using (11) were performed for the gamma and lognormal drop size distributions considered in the previous section.

Given the results of Fig. 3 one would expect significant integrated backscatter phase shifts δ_o at K_a band. Figure 4 shows the results of calculations of δ_o as a function of rain rate for $\lambda = 0.86$ cm. There is a lot of scatter because δ_o is related to R less directly than K_{DP}. For a given drop shape model, δ_o is related primarily to characteristic drop sizes (i.e., D_m in gamma distributions and D_g in lognormal distributions); it is less directly related to the widths of the distributions (i.e., n and σ) and not related to the normalizing factors (i.e., N_o and N_T). However, the general trend for δ_o is to increase as rain rate increases (due to the fact that larger rain rates are associated with larger drops). Accordingly as in the K_{DP} case, we approximated δ_o–R relations by power-law functions:

$$\delta^* = cR^d, \quad (12)$$

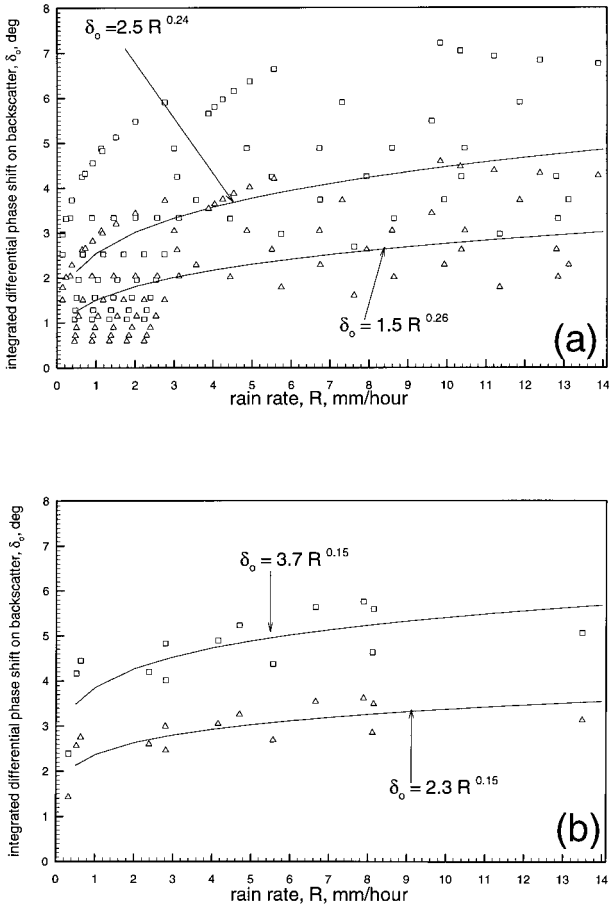

FIG. 4. Scatterplots of calculated backscatter differential phase shift vs rainfall rate, where $\lambda = 0.86$ cm: (a) gamma DSD and (b) lognormal DSD. Upper curves and squares are for the equilibrium drop shape; lower curves and triangles are for the mean drop shape.

where the coefficient c and the exponent d are presented in Fig. 4 (δ_o is in degrees and R is in mm h^{-1}).

As seen in Fig. 4, with an exception of a few data points, δ_o values at $\lambda = 0.86$ cm are less than 7°. These contributions to differential phase measurements can be comparable in magnitude if specific differential phase estimations are made over range intervals of several kilometers. Note that the backscatter differential phase at $\lambda = 0.86$ cm could reach 4°–5° even for very light precipitation ($R \approx 1$ mm h^{-1}).

Considerations expressed above indicate that K_{DP} estimates of rain rate in K_a band could be effective only for rather homogeneous light precipitations when DSD does not change significantly over sufficiently long estimation intervals, so that δ_o differences at the beginning and the end of the K_{DP} estimation interval are small. It should be noted also that backscatter phase shift contributions due to local changes in drop characteristic size could be evident as an isolated extremum in the generally increasing trend of φ_{DP} with range.

Alternatively, for short-range intervals and inhomogeneous precipitation, δ_o would dominate propagation

differential phase shifts, so differential phase measurements might be useful as estimators of hydrometer characteristic sizes (and possibly of shapes, with additional consideration of other polarization parameters), as suggested by Blackman et al. (1995) for melting-level studies.

Calculations performed for $\lambda = 3.2$ cm showed that δ_o values at X band are less than at K_a band by about one order of magnitude. The approximations (12) for $\lambda = 3.2$ cm are $0.3R^{0.5}$ and $0.18R^{0.5}$ for the gamma DSD and equilibrium and mean drop shapes, respectively. These results are in general agreement with earlier X-band assessments by Tan et al. (1991). These approximations demonstrate that differential backscatter phase shift is expected to be generally within about 1° for the rain-rate interval considered in this paper.

However, as previously mentioned, it is the difference in δ_o in the estimation interval [see (9)] that matters most, not the absolute values of δ_o (although local extrema in φ_{DP} due to backscatter can contaminate K_{DP} estimates as a slope of the total phase change with range). This difference is expected to be much smaller than 1° if DSD does not change drastically over the range interval used to estimate K_{DP}. Conceivably, a filtering approach (e.g., Hubert and Bringi 1995) can be used for the backscatter differential phase shift correction.

4. Experimental examples of K_{DP} measurements in rain at $\lambda = 3.2$ cm

The differential phase measurements of rain at $\lambda = 3.2$ cm were taken in September 1997 using the NOAA/ETL X-band radar. The radar was located at the Erie field site about 20 km northeast of Boulder, Colorado. The stratiform event of 20 September was associated with an atmospheric frontal passage and, depending on location, intermittent rain produced from 7 to 10 mm of water accumulation over 3 h. About 40% of the total rain was accumulated during a period between 0350 and 0440 UTC.

Measurements of φ_{DP} and other radar parameters were taken for radar beams that consisted of 256 range gates with the gate spacing of 150 m. The lowest elevation free of blockage and ground clutter was about 1.3°. For most of the event, the radar scanned inside the azimuthal sector from 90° to 310° at a rate of about 5° s^{-1} for two elevations (1.5° and 3°), so the time interval between the same azimuthal and elevation beam positions was about 1.5 min. Each ''beam'' of recorded radar data was based on averages from 64 consecutive HHVV transmitted sequences where H and V denote the transmission of horizontally and vertically polarized pulses.

Figure 5 shows an example of raw φ_{DP} measurements for one of the beams. These phase data are quite noisy; however, a positive trend of gradually increasing phase is apparent. No contributions of the backscatter differential phase shift were obvious in this dataset.

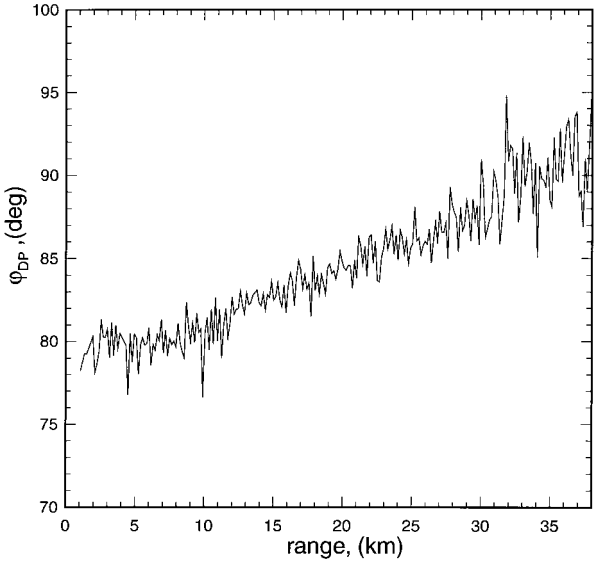

FIG. 5. An example of differential phase shift measurements (azimuth 187.5°, elev 1.5°, 0407:33 UTC 20 Sep 1997).

These raw phase data were subject to initial filtering, which included removal of artifacts (i.e., data points not associated with meteorological targets) by thresholding on Doppler velocities and normalized correlation coefficient between two consecutive echos. Near-zero Doppler velocity was suggestive of clutter-contaminated data, and the low correlation coefficient was an indicator of signals too weak to include. The K_{DP} values were then calculated as the slope of a linear regression line for sliding window intervals of range, as in Ryzhkov and Zrnic (1996). The regression window was shifted at increments of one range gate, and the resultant value of K_{DP} was assigned to the gate at the middle of the window. Larger window intervals are usually used for smaller K_{DP} values in order for a measurable phase change to be produced at the lighter rainfall rates. Here, we used intervals from 2 to 8 km to estimate the effect of the window size.

The data from six high-resolution rain gauges were available for comparisons with time series of rain accumulations retrieved from differential phase measurements. These tipping-bucket-type rain gauges were located along the different azimuthal directions at ranges from 2.75 to 21.74 km from the radar and provided resolution of 0.01″ for time series measurements of rain accumulation.

For purposes of illustration, Fig. 6 shows rainfall rates calculated from K_{DP} measurements as a function of time above one of the gauges located at a range of 11.46 km for 0350–0440 UTC. The measurements were taken at an elevation angle of 1.5°. Here R represents an average of rain rates calculated for three consecutive range gates and centered above the gauge location. Results calculated for different regression window intervals are presented in this figure. The K_{DP}–R relation obtained for

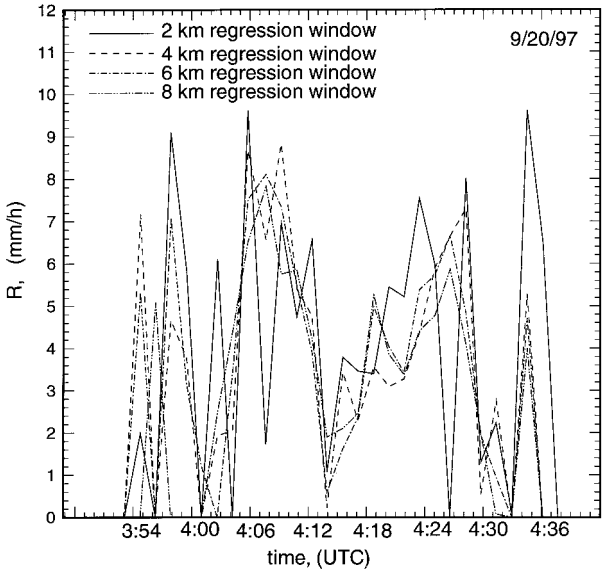

FIG. 6. Rainfall rate from K_{DP} measurements over the rain gauge located at azimuth 205.5° and range 11.46 km for different regression window intervals (K_{DP} data for $\beta = 1.5°$).

the mean drop aspect ratio ($R = 20.5K_{DP}^{0.80}$) was used to calculate rain rates. Note that the rain rates for different regression windows are quite close, except that data for the 2-km window exhibit more variability.

Time dependences of rainfall accumulation as derived from K_{DP} data and measured by this gauge are shown in Fig. 7. Accumulation values calculated using four different window intervals for K_{DP} are within about 20% of each other for this case (as was typical for other gauges) and they somewhat underestimate gauge measurements. The results for the longest regression window (8 km) differ the most, probably, because of the larger spatial averaging. Note that the equilibrium drop shape K_{DP}–R relation ($R = 14K_{DP}^{0.85}$) would provide accumulations smaller than those shown in Fig. 7 by a factor of about 1.6.

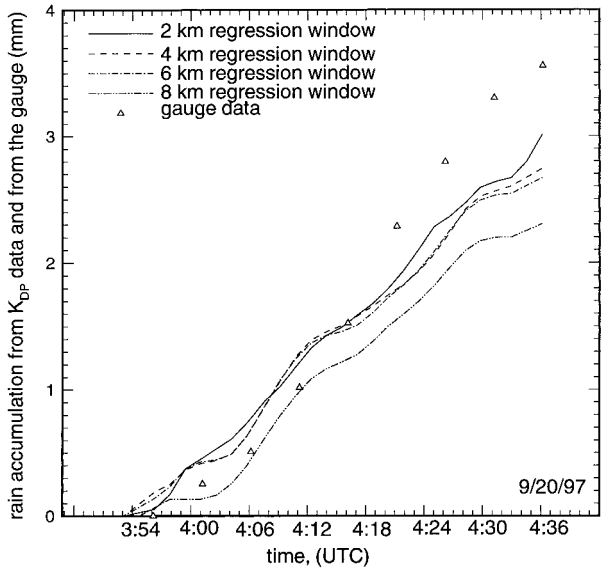

FIG. 7. Rain accumulation over the rain gauge at azimuth 205.5° and range 11.46 km for different regression window intervals (K_{DP} data for $\beta = 1.5°$).

Comparisons of radar data for the elevation 1.5° and ground measurements of rain accumulation (A) for all the gauges indicate that there is a very small mean (few percent) negative bias in radar estimates as compared to the gauge estimates if the relation $R = 20.5K_{DP}^{0.8}$ is used. Given uncertainty gauge measurements this bias can probably be neglected. The mean relative standard deviation (RSD) between radar and surface rain gauge datasets for all the gauges was about 39% (with variations of a few percentage points due to the choice of the regression window) for this rain event. RSD and the mean bias (B) were calculated using

$$\mathrm{RSD} = 100\%\left\{\sum_{i=1}^{N}[(A_i^{\mathrm{radar}} - A_i^{\mathrm{gauge}})/A_i^{\mathrm{gauge}}]^2/N\right\}^{0.5} \quad (13a)$$

and

$$B = 100\%\left\{\sum_{i=1}^{N}[(A_i^{\mathrm{radar}} - A_i^{\mathrm{gauge}})/A_i^{\mathrm{gauge}}]/N\right\}. \quad (13b)$$

For this rainfall event, the largest underestimation of gauge measurements by radar data was about a factor of 2 and the largest overestimation was about a factor of 1.5. The melting level was estimated to be at about 1.1 km, so radar rain estimates at elevation 1.5° were within the rain region for all the gauges. Comparisons of K_{DP}-derived rain accumulations at 1.5° and 3° elevations for the closest gauges, where 3° elevation rainfall estimates were still below the melting level, revealed a significant vertical variation in rain estimates for this event. Accumulation and rainfall rate data derived for the lower elevation were larger than those for the higher elevation by an average of 20%. This vertical variability of K_{DP} estimates of rain is not well understood now. It could contribute to a relatively high values of RSD.

The second stratiform rain event of the X-band K_{DP} field test was recorded on 23 September 1997. This event had a duration similar to the previous one; however, it produced smaller accumulations and was not as widespread as the event of 20 September. The radar was operating in an unattended mode inside the azimuthal sector from 90° to 310° for four consecutive elevations: 1.3°, 1.6°, 2°, and 2.3°. This scanning regime resulted in an approximately 3-min temporal resolution of radar estimates over the rain gauges.

Figure 8 shows rainfall rates derived from differential phase measurements for the gauge located at 15.61 km along the 187.5° azimuth. The data are presented for the lowest available elevation of 1.3° and, as before, the relation derived here for the mean aspect ratio of raindrops (i.e., $R = 20.5K_{DP}^{0.80}$) was used. As for the event

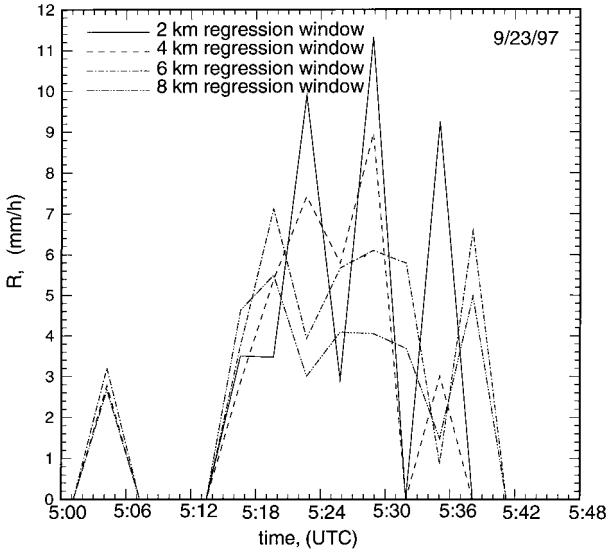

FIG. 8. Rainfall rate from K_{DP} measurements over the rain gauge located at azimuth 187.5° and range 15.61 km for different regression window intervals (K_{DP} data for $\beta = 1.3°$).

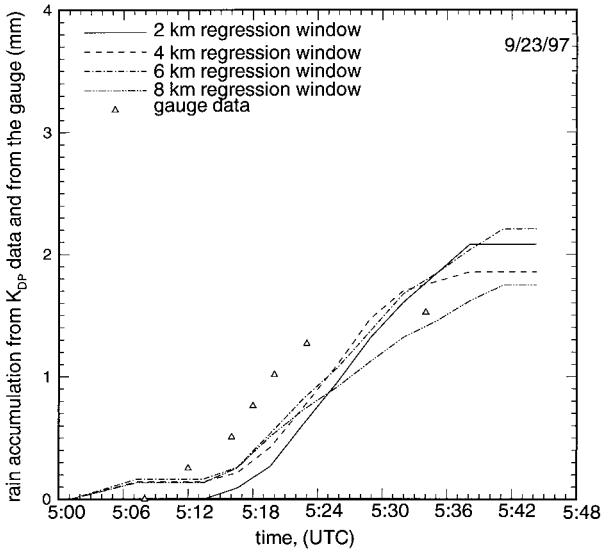

FIG. 9. Rain accumulation over the rain gauge at azimuth 187.5° and range 11.46 km for different regression window intervals (K_{DP} data for $\beta = 1.3°$).

of 20 September 1997, the 2-km regression window estimates exhibit the strongest temporal variability in retrieved rain rates. Generally, however, accumulation estimates derived with windows of different lengths agree relatively well, indicating that the rain was rather homogeneous horizontally.

Rain accumulations as a function of time for this gauge are presented in Fig. 9. As one can see, most of the liquid was accumulated over a 20-min time period. A time mismatch of several minutes between radar and gauge accumulations could result from a possible clock difference in these two instruments. Comparisons of the rainfall estimates for different radar elevations also revealed a vertical variability of rain that was not, however, as strong as for the previous event.

The mean bias and the relative standard deviation calculated as an average of four regression window intervals for this event (−6% and 38%, respectively) were very close to the values for the first event of 20 September 1997.

5. Conclusions

Prospects for estimating rainfall using differential phase shift (K_{DP}) measurements with X- and K_a-band radar were examined. It is shown that for rainfall rates of less than 15 mm h^{-1}, the possible backscatter differential phase shift δ_o at X band is usually less than about 1°. The backscatter differential phase shift contribution to K_{DP} measurements represents the difference in δ_o values at the edges of the range interval used for K_{DP} estimates and is expected to be smaller than K_{DP} values for such rain rates, especially if DSD does not change significantly over the estimation interval and several kilometers long intervals are used. Thus, this contribution usually should not introduce significant error into estimations of rainfall from K_{DP} measurements at X band in light and moderate rains. In marginal situations this contribution might be approximately corrected from retrieved rain rates.

The δ_o values at K_a band are approximately one order of magnitude larger than at X band, while the differential phase shifts due to propagation are only about two times larger. The relative strength of backscatter effects could prevent effective use of rain estimates using K_{DP} measurements at K_a band unless long-range intervals are used for rainfall estimations and the DSD does not vary significantly over these intervals.

Modeling K_{DP} for X and K_a bands showed that K_{DP}–R relations exhibit only modest variation due to variations in the parameters of gamma and lognormal drop size distributions. These relations, however, are very sensitive to the model of drop aspect ratio (a/b) as a function of drop size. The equilibrium aspect ratio ($a/b = 1.03–0.62D_e$) used in most studies for S band and the mean aspect ratio ($a/b = 1.03–0.44D_e$) used also here provide a factor of about 1.5 difference in K_{DP}–R relations for X band and a factor of about 2 difference for K_a band. Note, that the mean aspect ratio considered in this study was obtained by approximation of data from Kubesh and Beard (1993) for only the few data points that were published. This aspect ratio model, however, provides K_{DP}–R relations that are quite close (within 10%) to ones obtained for C band with the aspect ratio model reported by Keenan et al. (1997).

The X-band differential phase measurements of rain were conducted in September 1997 near Boulder, Colorado. Radar measurements were taken in a stratiform

event with intermittent rain averaging 4–5 mm h^{-1}. Data analysis showed that the lengths of the regression window intervals from 2 to 8 km used for K_{DP} estimation were providing close results in terms of rain accumulation (usually within 20%). This indicates a relative horizontal homogeneity of the observed rain and the possibility of getting a good spatial resolution of rain estimates for such light rainfalls. Note that the advantage of X-band wavelengths rather than longer wavelengths is its the ability to get a better resolution of estimates in light and moderate rains and/or to lower the limit (by about a factor of 3 compared with S band) of retrievable rain rates.

Comparisons of rain accumulations obtained from X-band differential phase measurements and by high-resolution rain gauges deployed in the area for two stratiform rain events yielded a small negative bias (few percent), with a relative standard deviation of about 38% for both cases if the relation for the mean drop aspect ratio is used: $R = 20.5K_{DP}^{0.80}$. In contrast, rain accumulations calculated with the relation for the equilibrium drop shape ($R = 14K_{DP}^{0.85}$) were lower by about a factor of 1.6 for these datasets.

The two events discussed above were the first experimental attempts to obtain quantitative rainfall assessments from K_{DP} measurements using the NOAA/ETL X-band radar. Subsequently, this radar participated in 1998 TRMM validation studies in Texas. Preliminary analysis for more intense rainfall ($R \sim 10$ mm h^{-1}) from these studies indicate that the K_{DP}–R relation based on the equilibrium drop shape, rather than the mean drop shape, could provide a better agreement between radar and gauge measurements. TRMM data will be reported in the future, but the different result underlines the need in ''tuning'' K_{DP}–R relations. More data are needed to better establish appropriate parameters of these relations at X band for different rain-rate intervals.

One factor that might have contributed to the difference between gauge comparison results obtained in Boulder and Houston is the difference in altitude of the experimental sites. Higher altitudes near Boulder (about 1600 m ASL) probably resulted in drop fall velocities greater than ones given by (7). Given that both K_{DP} and R depend on the details of DSD in a similar way, this may lead to the fact that a greater value of the coefficient a in K_{DP}–R relations was needed to reach better agreement with rain gauges. Since the terminal velocities of water drops are proportional approximately to the 0.45th power of the air density, ρ (Beard 1985), the coefficient a should then be considered as altitude dependent:

$$a = a_o(\rho_o/\rho)^{0.45}, \tag{14}$$

where the subscript o refers to sea level conditions.

It has been shown (e.g., Jameson 1994b; Ryzhkov and Zrnic 1995) that differential reflectivity measurements (Z_{DR}) can be used for tuning K_{DP}–R relations at S band. The coefficient a is proportional to some negative power of Z_{DR}. Since Z_{DR} is generally increasing with the rain rate, a decreases with an increase of R. Tuning Z_{DR}–R relations for both air density and Z_{DR} would bring data from Boulder and Houston into better agreement.

The situation at X band, however, is complicated by the differential attenuation affecting Z_{DR} measurements. It may be possible to resolve that problem with a scheme for correcting differential attenuation effects based on differential phase measurements. Such studies are, however, beyond the scope of current research.

Acknowledgments. We would like to acknowledge the efforts of the many participants who contributed to the data collection and analysis of these initial X-band measurements of propagation differential phase. K. Clark made many radar system upgrades over the last several years, and the development of ETL's new digital processor by C. Campbell was essential to this project. J. Gibson's display software allowed proper judgments about data quality to be made in real time. L. Church set up and maintained the network of rain gauges. I. Djalalova wrote software that allowed accessing to the data from the new signal processer. B. Bartram's dedication to the data collection phase is greatly appreciated. Funding from NOAA/ERL–USWRP was helpful in the initial stages of this work for implementing the differential phase capability in ETL's new radar processor. The X-band radar operations in Texas were funded by the NASA TRMM office and aided by cooperation from the city of Houston.

REFERENCES

Atlas, D., C. W. Ulbrich, and R. Meneghini, 1984: The multiparameter remote measurement of rainfall. *Radio Sci.,* **19,** 3–22.

Barber, P., and C. Yeh, 1975: Scattering of electromagnetic waves by arbitrarily shaped dielectric bodies. *Appl. Opt.,* **14,** 2864–2872.

Beard, K. V., 1985: Simple altitude adjustments to raindrop velocities for Doppler radar analysis. *J. Atmos. Oceanic Technol.,* **2,** 468–471.

Blackman, T. M., and A. J. Illingworth, 1997: Examining the lower limit of K_{DP} rain-rate estimation including a case study at S-band. Preprints, *28th Int. Conf. on Radar Meteorology,* Austin, TX, Amer. Meteor. Soc., 117–118.

——, ——, J. W. F. Goddard, and H. Sauvageot, 1995: Simultaneous differential phase measurements at 3 and 35 GHz. Preprints, *27th Int. Conf. on Radar Meteorology,* Vail, CO, Amer. Meteor. Soc., 464–466.

Bohren, C. F., and D. R. Huffman, 1983: *Absorption and Scattering of Light by Small Particles.* John Wiley and Sons, 530 pp.

Bringi, V. N., V. Chandrasekar, and R. Xiao, 1998: Raindrop axis ratios and size distributions in Florida rainshafts: An assessment of multiparameter radar algorithms. *IEEE Trans. Geosci. Remote Sens.,* **36,** 703–715.

Campbell, W. C., and J. S. Gibson, 1997: A programmable real-time data processing and display system for the NOAA/ETL Doppler radars. Preprints, *28th Int. Conf. on Radar Meteorology,* Austin, TX, Amer. Meteor. Soc., 178–179.

Chandrasekar, V., V. N. Bringi, V. N. Balakrishnan, and D. S. Zrnic, 1990: Error structure of multiparameter radar and surface measurements of rainfall. Part III: Specific differential phase. *J. Atmos. Oceanic Technol.,* **7,** 621–629.

Houze, R. A., Jr., and P. V. Hobbs, 1982: Organization and structure

of precipitating cloud systems. *Advances in Geophysics*, Vol. 24, Academic Press, 225–315.

Hubert, J., and V. N. Bringi, 1995: An iterative filtering technique for the analysis of copolar differential phase and dual-frequency radar measurements. *J. Atmos. Oceanic Technol.,* **12,** 643–648.

Jameson, A. R., 1991: A comparison of microwave techniques for measuring rainfall. *J. Appl. Meteor.,* **30,** 32–54.

——, 1994a: An alternative approach to estimating rainfall rate by radar using propagation differential phase shift. *J. Atmos. Oceanic Technol.,* **11,** 122–131.

——, 1994b: Measuring rainwater content by radar using propagation differential phase shift. *J. Atmos. Oceanic Technol.,* **11,** 299–310.

Keenan, T. D., D. Zrnic, L. Carey, P. May, and S. A. Rutledge, 1997: Sensitivity of C-band polarimetric variables to propagation and backscatter effects in rain. Preprints, *28th Int. Conf. on Radar Meteorology,* Austin, TX, Amer. Meteor. Soc., 13–14.

Kezys, V., E. Torlaschi, and S. Haykin, 1993: Potential capabilities of coherent dual-polarization X-band radar. Preprints, *26th Int. Conf. on Radar Meteorology,* Norman, OK, Amer. Meteor. Soc., 106–108.

Kubesh, R. J., and K. V. Beard, 1993: Laboratory measurements of spontaneous oscillations for moderate-size raindrops. *J. Atmos. Sci.,* **50,** 1089–1098.

Matrosov, S. Y., 1991: Theoretical study of radar polarization parameters obtained from cirrus clouds. *J. Atmos. Sci.,* **48,** 1062–1070.

May, P. T., T. D. Keenan, D. S. Zrnic, and L. Carey, 1997: Polarimetric measurements of rain at a 5 cm wavelength: Comparisons with rain gauge measurements. Preprints, *28th Int. Conf. on Radar Meteorology,* Austin, TX, Amer. Meteor. Soc., 127–128.

Mazin, I. P., Ed., 1989: *Handbook of Clouds and Atmosphere.* Gidrometeoizdat, Leningrad, 648 pp.

Morrison, J. A., and M. J. Cross, 1974: Scattering of a plane electromagnetic wave by axisymmetric raindrops. *Bell Syst. Tech. J.,* **52,** 955–1019.

Pruppacher, H. R., and R. L. Pitter, 1971: A semi-empirical determination of the shape of cloud and rain drops. *J. Atmos. Sci.,* **28,** 86–94.

Ryzhkov, A. V., and D. S. Zrnic, 1995: Comparison of dual-polarization radar estimators of rain. *J. Atmos. Oceanic Technol.,* **12,** 249–256.

——, and ——, 1996: Assessment of rainfall measurement that uses specific differential phase. *J. Appl. Meteor.,* **35,** 2080–2090.

Sachidananda, M., and D. S. Zrnic, 1987: Rain rate estimates from differential polarization measurements. *J. Atmos. Oceanic Technol.,* **4,** 587–598.

Sauvageot, H., and J. P. Lacaux, 1995: The shape of averaged drop size distributions. *J. Atmos. Sci.,* **52,** 1070–1083.

Seliga, T. A., and V. N. Bringi, 1978: Differential reflectivity and differential phase shift: Applications in radar meteorology. *Radio Sci.,* **13,** 271–275.

Tan, J., A. R. Holt, A. Hendry, and D. H. O. Bebbington, 1991: Extracting rainfall rates from X-band CDR radar data by using differential propagation phase shift. *J. Atmos. Oceanic Technol.,* **8,** 790–801.

Ulbrich, C. W., 1983: Natural variations in the analytical form of the raindrop distribution. *J. Climate Appl. Meteor.,* **22,** 1764–1775.

Wobus, H. B., F. W. Murray, and L. R. Koenig, 1971: Calculation of the terminal velocity of water drops. *J. Appl. Meteor.,* **10,** 751–754.

Zrnic, D. S., and A. V. Ryzhkov, 1996: Advantages of rain measurements using specific differential phase. *J. Atmos. Oceanic Technol.,* **13,** 454–464.